Journal of Magnetics 10(1), 23-27 (2005)

Crystallographic Effects of Larger Indium Ion Substitution in $NiFe_{2-x}In_xO_4$ ($x = 0$, 0.2, 0.5, and 1.0) System

Sunghyun Yoon*, Chang Sun Yoon and Byung Ho Kim

Dept. of Physics, Gunsan National University, Gunsan 573-701, Korea

(Received 7 March 2005)

The crystallographic and magnetic properties of a series of substitutions in nickel ferrite where the Fe^{3+} is replaced with In^{3+} have been investigated using X-ray diffraction (XRD) and Mössbauer spectroscopy. Information on the exact crystalline structure, lattice parameters, bond lengths and bond angles were obtained by refining their XRD profiles by a Rietveld method. All the crystal structures were found to be cubic with the space group *Fd/3m*. The lattice constants increased with In^{3+} concentration. The expansion of the tetrahedron was outstanding, indicative of the tetrahedral (A) site preference of larger indium ion. The Mössbauer spectra showed two sets of sextuplet originating from ferric ions occupying the tetrahedral sites and the octahedral (B) sites under the Néel temperature T_N. Regardless of the composition x, the electric quadrupole splitting was zero within the experimental error. At $x = 0.2$, the magnetic hyperfine fields increased slightly, which meant that the nonmagnetic indium ions occupied preferentially the A-site. At the same time, the intensity of the B-site subspectra decreased markedly at the elevated temperature, indicating that the occupation of the A site by indium induced a considerable perturbation on the B site.

Key words : Spinel, Cation Distribution, Mössbauer Spectroscopy

1. Introduction

Thorough interpretations on the magnetic properties of oxides having the spinel structure are not possible without the determination of their cation distributions [1]. In this respect, ^{57}Fe Mössbauer spectroscopy is a powerful method because this technique is able to elucidate the local structure through hyperfine interactions. It is well known that In^{3+} and Ni^{2+} prefer the tetrahedral (A) sites and the octahedral (B) sites, respectively in the spinel structure [2]. Krishnan and Cagan performed a magnetic moment measurement for the system $NiFe_{2-x}In_xO_4$ and reported that for $x < 0.25$, In^{3+} ions enter the A sites but for higher values x enter the B sites [3]. As the indium concentration was increased, the experimental magnetic moment deviated from a value calculated by the Néel model at $x = 0.25$. At $x > 0.25$, the measured magnetic moment was decreased with the indium substitution.

Indium has a relatively large ionic radius. Now it will be of interest to investigate the effect of the substitution of ions having greater ionic radii on the crystal structure and the ionic distribution. However, the exact crystallographic aspects of the indium substitution have not been reported yet. The present paper will report upon the effect of larger indium ion substitution on the crystallographic and magnetic properties.

*Corresponding author: Tel: +82-63-469-4562,
Fax: +82-63-469-4561, e-mail: shyoon@kunsan.ac.kr

2. Experiment

The $NiFe_{2-x}In_xO_4$ compounds ($x = 0$, 0.2, 0.5, and 1.0) were prepared by using the conventional ceramic method, starting with NiO, Fe_2O_3, and In_2O_3 powders. A mixture of appropriate proportions of the compounds was ground and press-molded into a pellet. In order to prevent an unwanted evaporation of In_2O_3, the pellet was first heated to 830 °C, kept at this temperature for 1 day, heated further at 1100 °C for 2 days, and then slowly cooled down to room temperature at the rate of 10 °C/hour. This process was repeated in order to obtain a homogeneous material. At $x = 1.0$, there appear tiny traces of In_2O_3, which cannot be removed even after a prolonged firing. Pure spinel phase could be obtained by the sintering at 1300 °C. X-ray diffraction (XRD) patterns of the samples were obtained with Cu Kα radiation. The XRD patterns at room temperature were taken at a slow scanning speed

(0.5° advance in 2θ per min.) to enhance the resolution. A Mössbauer spectrometer of conventional transmission type was then used in constant-acceleration mode. ^{57}Co source in an Rh matrix was used at room temperature.

3. Results and Discussion

An analysis of the XRD patterns indicates that the structure of the samples should be a cubic spinel, showing no marked changes with composition. Profile refinements are carried out using the GSAS program package [4] in space group *Fd/3m* with the assumption that all the nickel ions occupy the octahedral site. Since $NiFe_2O_4$ is known to crystallize in the inverse spinel structure, this structural assumption is quite reasonable. In the process of refinement, we also assume that there are no orderings in cations of both sites. A profile function formed by a convolution of a pseudo-Voigt shape (CW profile #2 provided in the package) is used. The final observed and calculated room-temperature XRD profiles for the samples are illustrated in Fig. 1. The results of the refinement are summarized in Table 1.

Lattice constants increase as the Fe^{3+} ions are substituted by the In^{3+} ions. This is consistent with the fact that ionic radius for In^{3+} (0.93 Å) is larger than that for Fe^{3+} (0.74 Å) [5]. Bond distances Fe(A)-O, and Fe(B)-O all increase monotonically with increasing indium content. However, the increasing trend for the Fe(A)-O distance is the steepest among them. This indicates that indium ions are mainly entering the A sites. Bond angle O-Fe(A)-O maintains 109.47°, which means that FeO_4 tetrahedron is not distorted with the substitution of indium. On the other hand, FeO_6 octahedron is slightly distorted in view of the fact that O-Fe(B)-O angles in the octahedron deviate

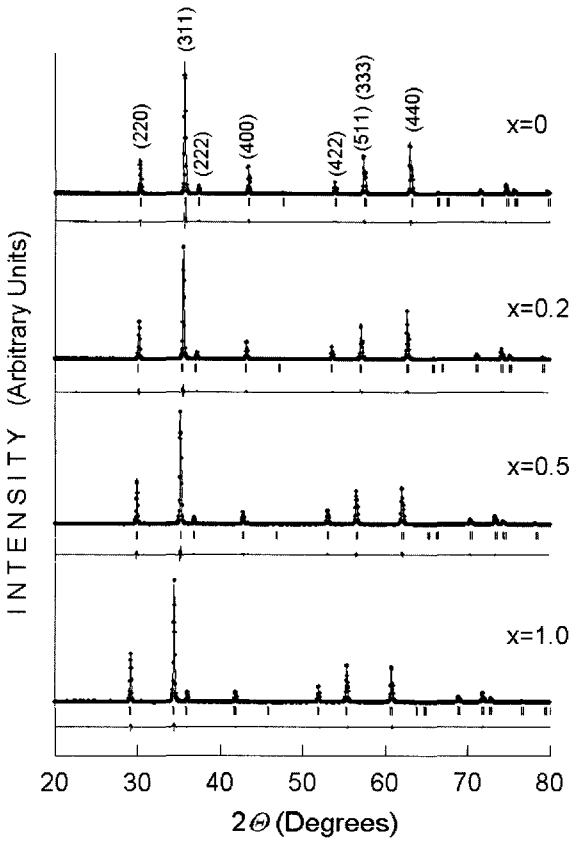

Fig. 1. XRD profiles, calculated and difference curves of $NiFe_{2-x}In_xO_4$ at room temperature.

Table 1. Structural parameters, bond distances, bond angles and thermal factors for $NiFe_{2-x}In_xO_4$ at room temperature. (Space group: *Fd/3m*)

x		0.0	0.2	0.5	1.0
Lattice constant a (Å)		8.316	8.372	8.458	8.558
Oxygen position x_O		0.2563	0.2569	0.2585	0.2538
Bond distances (Å)	Fe(A)-O	1.891	1.913	1.955	1.982
	Fe(B)-O	2.028	2.037	2.045	2.075
Bond angles (°)	O-Fe(A)-O	109.47	109.47	109.47	109.47
	O-Fe(B)-O	180.0 87.0 93.0	180.0 86.7 93.3	180.0 85.9 94.1	180.0 86.0 94.0
	Fe(A)-O-Fe(B)	123.2	123.0	122.4	122.5
	Fe(B)-O-Fe(B)	92.9	93.2	93.9	93.9
Thermal factors (Å^2)	$u_A \times 100$	1.641	2.052	1.842	2.363
	$u_B \times 100$	1.684	1.590	1.837	2.515
	$u_O \times 100$	2.217	2.227	2.515	2.693
Cation compositions		$[Fe]_A\ (NiFe)_B$	$[Fe_{0.8}In_{0.2}]_A\ (NiFe)_B$	$[Fe_{0.62}In_{0.38}]_A$ $(NiFe_{0.88}In_{0.12})_B$	$[Fe_{0.41}In_{0.59}]_A$ $(NiFe_{0.58}In_{0.42})_B$

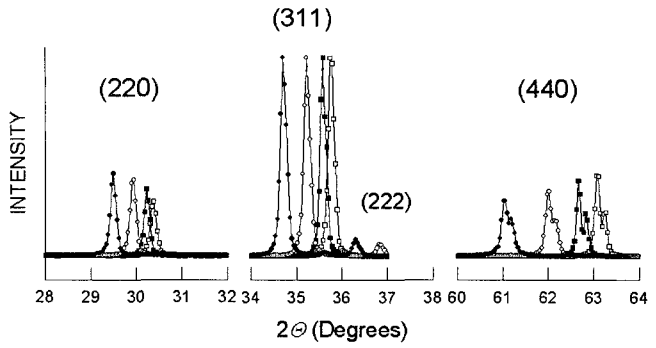

Fig. 2. Variation of three dominant peaks in the XRD patterns for the $NiFe_{2-x}In_xO_4$ (x = 1.0, 0.5, 0.2, and 0 from left to right).

gradually from 90° with the increase of the indium concentration. This is consistent with the fact that oxygen parameters x_O also increase, which means that a tetrahedron expands in order to accommodate the bigger indium ion. A close examination of the spinel crystal structure reveals that this expansion of a tetrahedron has to involve a perturbation of the neighboring octahedral sites. Cation distributions deduced from the refinements of XRD profiles are also given in the bottom row of Table 1.

Figure 2 shows the composition dependencies of three dominant peaks in the XRD patterns for the $NiFe_{2-x}In_xO_4$ (x = 0, 0.2, 0.5, and 1.0) samples taken at room temperature. When the XRD profiles are normalized so that the maximum (311) peaks have equal intensities, (220) peaks in the lower angle region grow as the indium content x increases. On the other hand, intensities of the (440) peaks in the higher angle region decrease with the increase of indium content. It is apparent that there is a greater decrease in the reflected intensity at high angles than at low angles as the indium content x increases. In the intensity calculations this effect can be explained by introducing the temperature factor $e^{-2u_{iso}}$ in the atomic structure factor. u_{iso} is defined as the isotropic thermal factor. For a constant temperature, the greater the thermal factor u_{iso}, the greater decrease in the intensity at high angles than at low angles would result. Put these all together, it is very likely that the u_{iso} increases as the indium concentration increases. This can be seen actually in the Table 1. u_A, u_B, and u_O correspond to the thermal factors for the A-, B-, and oxygen sites, respectively. Qualitatively, a temperature factor decreases as 2θ increases. In the case of cubic crystal structure, Debye has given the following expression:

$$u_{iso}=\frac{6h^2T}{mk_B\Theta^2}\left[p(x)+\frac{x}{4}\right]\left(\frac{\sin\theta}{\lambda}\right)^2,$$

Table 2. The Néel temperatures T_N and the Debye temperatures Θ deduced from XRD and Mössbauer spectroscopy (MS)

x			0	0.2	0.5	1.0
T_N (K)			860	810	590	310
Θ (K)	by XRD	A	220	195	207	184
		B	217	205	208	174
	by MS	A	481	364	242	–
		B	478	251	180	–

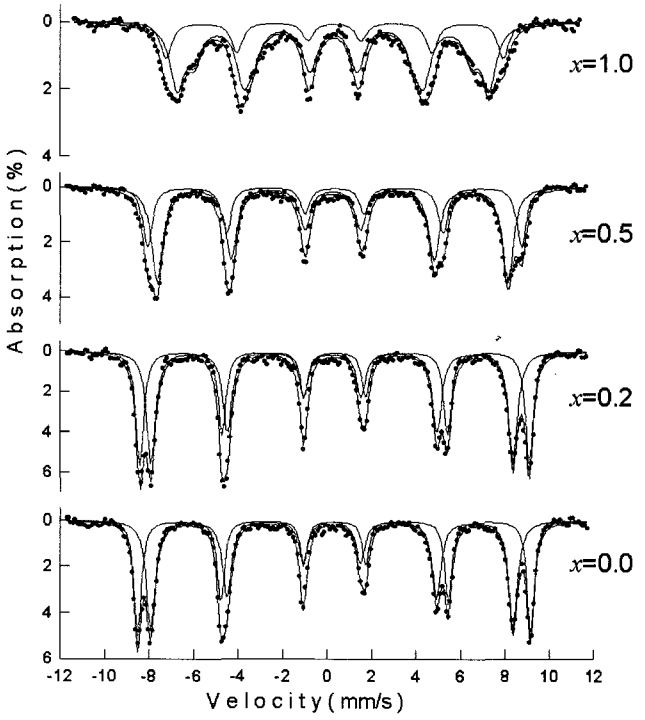

Fig. 3. Mössbauer spectra of $NiFe_{2-x}In_xO_4$ (x = 0, 0.2, 0.5, and 1.0) at 80 K.

where h is Planck's constant, T the absolute temperature, m the mass of the atom, k_B Boltzmann's constant, Θ the Debye characteristic temperature, $x = \Theta/T$, and $p(x)$ is a function tabulated in Ref. [6]. From the values of u_A and u_B in the Table 1, we can calculate the Debye temperature for the A site and the B site. These are listed in Table 2. These will be compared with the Debye temperatures deduced from the Mössbauer spectroscopy later.

Figures 3 and 4 illustrate Mössbauer spectra taken at absorber temperature of 80 K and 300 K, respectively. Typical hyperfine parameters at 80 K and 300 K are listed in Table 3. At 80 K, the Mössbauer spectra compose two sets of sharp six-line pattern except for the case of x = 1.0. As the temperature rises, the spectra become broad increasingly with the increase of indium concentration. This asymmetric broadening of the Mössbauer spectral

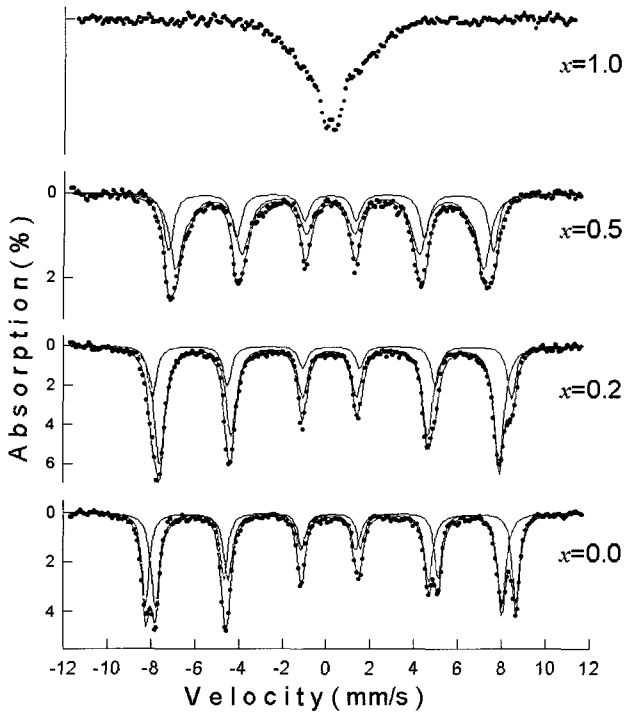

Fig. 4. Mössbauer spectra of $NiFe_{2-x}In_xO_4$ ($x = 0$, 0.2, 0.5, and 1.0) at 300 K. No attempt was made to fit the spectra for $x = 1.0$ due to the heavy overlap.

lines may result from both the distribution of the possible environments for an iron sites and the different temperature-dependencies of the magnetic hyperfine fields at various iron sites. The same explanation was given to the analysis of Mössbauer spectra for spinel system $CuFe_{2-x}Cr_xO_4$ [7].

While both the lattice parameters and the Néel temperatures (see Table 2) show monotonic dependencies with indium content, hyperfine field values at low temperature show a departure from this variation at $x = 0.2$. Hyperfine field at the A site even increases slightly as the non-magnetic indium content increases from $x = 0$ to $x = 0.2$. This can seemingly be attributed to the predominance of the negative B-B interaction or to the formation of non-collinear spin structure due to a diamagnetic substitution. However, the magnitude of $J_{B\text{-}B}$ is known to be much smaller than that of $J_{A\text{-}B}$ in the $NiFe_2O_4$ [8]. Furthermore, since it was already found that $NiFeInO_4$ had a collinear spin structure [9], the two possibilities can be ruled out. Taking into account of the fact that indium prefers the A site, however, this can be explained by assuming that there might occur a change in indium distribution among the sites near $x = 0.2$. To be more specific, the concentration of indium in the A site reaches its maximum, and indium begins to enter the B sites when $x > 0.2$. This is partly consistent with the steeper variation of bond distances for the A site as mentioned above.

The most remarkable change in Mössbauer spectra is that the intensity of the B-site subspectra decreases more rapidly than that of the A-site subspectra as the indium content increases. This behavior is most outstanding in the case of $x = 0.2$. An experimental absorption area for a component spectrum should be closely related to both the recoil-free fraction of the corresponding site and the distribution of iron ions. Area ratios I_A/I_B at 80 K and 300 K are listed in Table 3. The Debye model gives the following expression for the recoil-free fraction:

$$f=\exp\left[-\frac{3E_R}{2k_B\Theta}\left(1+\frac{4T^2}{\Theta^2}\int_0^{\Theta/T}\frac{x\,dx}{e^x-1}\right)\right],$$

where E_R is the recoil energy of ^{57}Fe nucleus for the 14.4 keV gamma ray. Θ and k_B represent the Debye temperature and the Boltzmann constant, respectively. The Debye temperature of each site was determined from the temperature dependence of the experimental absorption area in the low temperature region where the spectra were well resolved. Results of the analysis are summarized in Table 2. In the case of $NiFe_2O_4$, the values for the tetrahedral and the octahedral sites are found to be Θ_A = 481 K and Θ_B = 478 K, suggesting atomic binding forces of nearly equal strengths for both sites. However, as the indium content increases, Debye temperature gradually

Table 3. Magnetic hyperfine fields H_{hf}, isomer shifts δ, and the intensity ratios for the tetrahedral (A) and the octahedral (B) sites at 80 K and 300 K in $NiFe_{2-x}In_xO_4$

x		0		0.2		0.5		1.0	
site		A	B	A	B	A	B	A	B
80 K	H_{hf} (T)	50.6	54.7	50.8	54.6	49.0	52.3	45.8	48.1
	δ(mm/s)	0.21	0.34	0.23	0.35	0.24	0.34	0.24	0.36
	I_A/I_B	1.13		1.14		1.84		2.97	
300 K	H_{hf} (T)	49.2	52.6	49.2	51.8	43.0	45.8	–	–
	δ(mm/s)	0.12	0.24	0.16	0.25	0.16	0.23	–	–
	I_A/I_B	1.20		2.77		2.06		–	

decreased. As a whole, Θ_B is lower than Θ_A, indicating that the B sites are considerably perturbed. In comparing these with the values determined from the XRD analysis, however, the results from the XRD are not consistent with those from the Mössbauer spectroscopy. This might reflect the fact that interaction of gamma ray is more intensively affected by atomic thermal vibration than that of X-ray. Furthermore, XRD is not a sensitive method enough to distinguish the various metal ions. On the other hand, Mössbauer spectroscopy is a method exclusively effective on the iron ions.

From the values of isomer shift listed in Table 3, it is apparent that the charge state of iron ion is trivalent. It is also clear that *s*-electron density at the ^{57}Fe nucleus is not affected by the indium substitution. Quadrupole splitting values are zero within experimental errors for all the samples in the whole temperature range examined. It means that the electronic environmental symmetry is not so much altered by the indium substitution.

4. Conclusion

The effects of the larger indium ion substitution on the crystallographic and magnetic properties of the $NiFe_{2-x}In_xO_4$ system have been studied by XRD and Mössbauer spectroscopy. As the In^{3+} content was increased, the tetrahedron expanded more rapidly than the octahedron did. This is a consequence of the tetrahedral site preference of the indium ions. The occupation of the larger indium ions on the A sites in turn induced a structural perturbation on the neighboring octahedral sites, which was observed by both the XRD patterns and the Mössbauer spectra. The fraction of the indium ions on the A site was the maximum when $x = 0.2$, beyond which the indium ions began to occupy the B sites.

Acknowledgement

This work was supported by the Korea Science and Engineering Foundation under Grant No. R05-2001-000-00128-0.

References

[1] Hyunsook Lee, Jae-Gwang Lee, K. S. Baek, and H. N. Oak, J. Magnetics **8**(4), 138 (2003).
[2] L. R. Maxwell and S. J. Pickart, Phys. Rev. **96**, 1501 (1954).
[3] R. Krishnan and V. Cagan, IEEE Trans. Magn. **7**, 613 (1971).
[4] A. C. Larson and R. B. von Dreele, *Gensral Structure Analysys System*, Report No. LAUR-86-748, Los Alamos National Laboratory, Los Alamos, (1990).
[5] R. D. Shannon and C. T. Prewitt, Acta Cryst. B **25**, 925 (1969).
[6] B. D. Cullity, *Elements of X-Ray Diffraction*, 2nd ed., Addison Wesley, Massachusetts, (1978) p. 526.
[7] H. N. Oak, K. S. Baek, and E. J. Choi, Phys. Rev B **40**, 84 (1989).
[8] S. Krupicka and P. Novak, *Ferromagnetic materials*, North Holland, Amsterdam, (1982) pp. 216-220.
[9] R. Gerardin, A. Alebouyeh, J. F. Brice, O. Evrado, and J. P. Sanchez, J. Solid State Chem. **76**, 398 (1988).